Journal of Glaciology

Article

Cite this article: Pickell DJ, Hawley RL (2024). Performance characterization of a new, low-cost multi-GNSS instrument for the cryosphere. *Journal of Glaciology* 1–7. https://doi.org/10.1017/jog.2023.97

Received: 23 June 2023
Revised: 3 November 2023
Accepted: 9 November 2023

Keywords:
glacier mapping; glaciological instruments and methods; glacier monitoring; snow/ice surface processes

Corresponding author:
Derek J. Pickell;
Email: derek.gr@dartmouth.edu

cambridge.org/jog

Performance characterization of a new, low-cost multi-GNSS instrument for the cryosphere

Derek James Pickell and Robert Lyman Hawley

Department of Earth Sciences, Dartmouth College, Hanover, USA

Abstract

We developed a multi-frequency, multi-Global Navigation Satellite System (GNSS) positioning instrument optimized for autonomous applications in the cryosphere. At lower power requirements and a fraction of the cost and weight compared to commercially available options, this instrument simplifies field usage and associated logistics. In this paper, we assess several baseline aspects of performance in a polar environment relative to geodetic receivers commonly used for glaciological applications. Evaluations of precision and relative accuracy of positioning show millimeter to centimeter-level ('geodetic-grade') quality of this instrument, making it a competitive alternative for GNSS glaciological and geophysical applications such as monitoring surface elevation change and ice flow. An array of these instruments, tested in the field on the Greenland Ice Sheet, also demonstrated robustness throughout the polar winter and met power and reliability requirements.

1 Introduction

The precise determination of position with Global Navigation Satellite Systems (GNSS) allows glaciologists to measure ice velocity, strain, firn densification, surface elevation change and isostatic uplift, which together help illuminate the state of the world's glaciers and ice sheets (e.g. King, 2004). The use of GNSS instrumentation in the cryosphere spans back to the 1980s during the advent of the Global Positioning System (GPS), which expanded researchers' reach into remote regions where traditional survey methods were often impractical (e.g. Möller and Ritter, 1988). With a reliable and growing network of positioning satellites, GNSS instruments have become a fundamental glaciological tool for precise positioning. These capabilities, combined with precision and accuracy now at millimeter-level and sample rates in excess of 1 Hz, have led to new use cases in glaciology. Recent studies have employed GNSS data for quantifying ice mass loss by detecting proximal bedrock uplift (Hansen and others, 2021), providing Arctic atmospheric insights (Mitchell and others, 2005), measuring snow accumulation using interferometric reflectometry (Larson and others, 2020) and validating space-based measurements (Brunt and others, 2021).

Despite these advances, the primary drawback of GNSS technology, and especially commercial-off-the-shelf (COTS) instruments, is that relatively large power requirements conflict with the need to run these instruments through polar winters in static configurations or as a part of kinematic traverses, complicating field logistics with burdensome and costly power systems. While some studies have employed COTS receivers in the field (e.g. Khan and others, 2022; Still and others, 2022), and others have made power-minimizing design or configuration modifications in their deployments (e.g. Dunse and others, 2012), a full multi-band, multi-constellation, lightweight and cost-effective alternative optimized for the cryosphere can both vastly simplify deployment and allow for more extensive or capable cryosphere GNSS applications (Jones and others, 2016).

With the continued miniaturization and power reduction of original equipment manufacturer (OEM) GNSS modules, coupled with multi-constellation and multi-band tracking capabilities, this technology now enables centimeter or millimeter-level positioning at a reduced unit cost. Here, we developed a GNSS instrument that integrates this new generation of OEM receiver technology alongside a logging system, microcontroller, low-cost multi-GNSS antenna and power circuitry. While the potential geophysical applications of this technology are numerous, we focused on developing a system that will enable research in the cryosphere, and specifically within icy, remote environments where GNSS networks or campaigns can be rapidly carried out by small research teams. We also emphasize the ability to enable multi-constellation and multi-frequency tracking, along with logging raw GNSS data such as carrier and phase measurements akin to other geodetic receivers, which broaden the use-cases of this instrument into areas such as ionospheric monitoring and interferometric reflectometry studies. The instrument system is henceforth referred to as Open GNSS Research Equipment (OGRE). In this paper, we describe the OGRE design and evaluate the degree to which we meet low-power and reliability criteria in a cold environment, while also quantifying OGRE performance in enabling the collection of scientific-quality data.

2 Instrument design

2.1 Overview

The OGRE (Fig. 1) was designed to minimize power consumption, be simple and reliable in the field and be a low-cost alternative to commercial geodetic receivers. All components are surface-mounted onto a two-layer printed circuit board (PCB), including the u-blox ZED-F9P GNSS receiver module, a Sparkfun Artemis/Ambiq Apollo3 microcontroller unit (MCU), a microSD card slot and other peripheral and power circuitry (Fig. 2). At the time of the writing of this manuscript, the material cost of the OGRE instrument (not including the antenna or other external components) totaled 200 USD. All electrical schematics and hardware manufacturing files are provided alongside the device firmware on www.github.com/glaciology/OGRENet as part of an open-source initiative to make our work easily adaptable and reconfigurable.

The reasons for the selection of the ZED-F9P as the receiver module include multi-band and multi-constellation tracking capabilities (GPS-L1C/A and L2C, Beidou-B1I and B2I, Galileo-E1B/C and E5b, Glonass-L1OF and L2OF), a low cost relative to existing commercial geodetic modules, an extensive and engaged scientific and general user community and relatively low-power consumption (Table 1). Other projects making use of the ZED-F9P show near-geodetic grade positioning, with centimeter or millimeter displacement detection possible even when coupled with a low-cost antenna (Hamza and others, 2021, e.g.).

The microcontroller, built on a Cortex-M4F core, governs the GNSS module configuration and data flow, controls power supplies to the peripheral modules, buffers and processes raw GNSS data at a low level for logging to a microSD card and measures and monitors diagnostic status such as internal temperature, battery supply and hardware faults. The MCU offers a variety of programming methods at various abstraction levels, but the firmware can be modified at a high level in the Arduino development environment, optimized for ease of use.

2.2 Instrument configuration and logging

The OGRE is configured by a user-provided CONFIG.txt file that is read from the microSD card, or by default hard-coded values within the firmware when a configuration file is not provided by the user. The following options are definable:

Data log duration: (1) continuously, (2) daily or daily for a specified interval, (3) monthly on a specific day, for 24 h, or (4) for a certain time duration on any number of user-specified dates marked on a date file input to the microSD.
Data log interval: numeric value in seconds, with 1 representing 1 s, 15 representing 15 s, etc.
Constellations to enable: GPS, GLONASS, BEIDOU, GALILEO, QZSS and Satellite Navigation Messages.
Power options: (1) enable the battery voltage monitoring system, (2) disable LED indicator lights to save additional power.

Raw GNSS data, including pseudorange measurements, carrier phase, Doppler and signal to noise ratios, are logged in the u-blox binary format (.ubx) to the microSD card, alongside a corresponding debug file that contains vital device information such as battery voltage, MCU internal temperature and any read/write errors. We estimate that under open sky conditions, the receiver will generate 22 GB of uncompressed data from logging GPS L1/L2 raw 1 Hz data and corresponding navigation messages for a continuous year, which would fit comfortably onto a standard 32GB microSD card. When or if the OGRE is configured to not log data, or if the battery voltage falls beneath a specified value, it enters a low-power state of approximately 1 mW.

Figure 1. OGRE in 6.75 × 6 × 2.75 cm 3D-printed housing with lid removed. For field applications, we place this assembly inside a waterproof housing with bulkhead connections to the antenna and battery.

2.3 Additional specifications and external interface

The OGRE features a screw terminal for quick connection to an external battery. For all our testing, we used a 12 V lead acid advanced glass mat (AGM) battery, but input voltages to the OGRE can range from 6 to 20 V. In addition to the battery interface, we also incorporated a variety of dedicated digital or analog input and output pins and externally accessible UART, SPI and I2C buses that are user-configurable in the firmware for the integration of external modules such as data telemetry hardware or additional sensors. Finally, an SMA connector is mounted to the PCB for connection to a powered 3.3 V active antenna. In this study, we pair the instrument with two low-cost multi-frequency and multi-constellation antennas: a patch style u-blox ANN-MB with an external ground plane for the kinematic evaluations, and a survey-style TOPGNSS TOP106 for the static applications.

3 Field performance and evaluation

3.1 Field site and performance overview

The Summit region of the Greenland Ice Sheet (72.573 N 38.470 W, 3247 m ASL) provides an ideal testing location for GNSS glaciological equipment given its lack of sky obstructions and well-studied environment with industry-standard GNSS and GPS receivers. With a daily mean temperature around −40°C during the coldest months and average wind speeds in excess of 5 m s^{-1} in the winter, we assess environmental performance in battery robustness and instrument reliability (Castellani and others, 2015). We established a 12-station array of OGREs over a 40 km by 8 km grid that autonomously operated over the course of a year, providing insights into these environmental metrics. All stations were deployed within a 3 d period during the summer of 2022 and data were retrieved the following year.

For kinematic data quality assessments, we conducted several 15 km transect surveys with both an OGRE and a Trimble R7 receiver. A series of long-term, continuously operated, fixed GNSS stations have also been installed on various Summit Station buildings since 2009, with the most recent iteration

https://doi.org/10.1017/jog.2023.97 Published online by Cambridge University Press

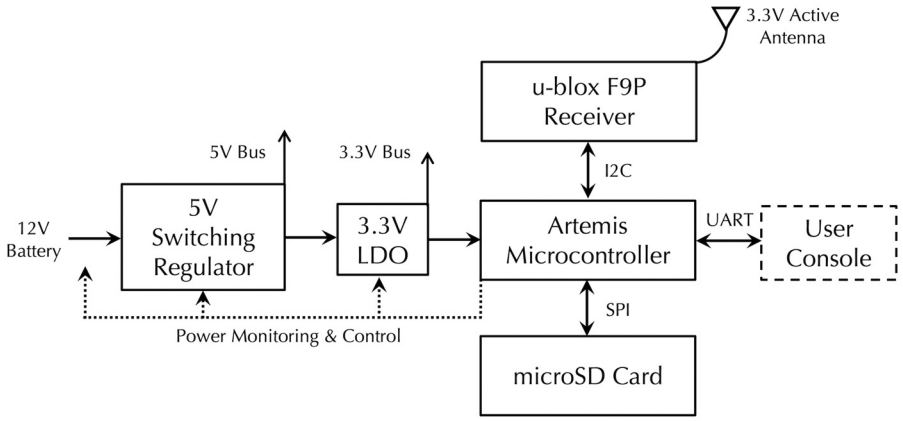

Figure 2. System diagram with principal components.

Table 1. Various GNSS receiver power requirements with maximum number of constellations enabled during tracking: (A) OEM GNSS receiver modules, (B) COTS receivers used for comparison in this paper and (C) OGRE (this paper), with integrated ZED-F9P, logging 1 Hz to microSD with all constellations enabled

	Instrument	Power (W)
(A)	u-blox ZED-F9P[a]	0.26
	Trimble BD99x[b]	1.50
	Skytraq PX1122R[c]	0.33
	Septentrio AsteRx-m[d]	0.95
(B)	Trimble NetR9[e]	3.8
	Trimble R7[f]	4.0
(C)	OGRE	0.63

[a] https://content.u-blox.com/sites/default/files/ZED-F9P-04B_DataSheet_UBX-21044850.pdf
[b] https://info.intech.trimble.com/bd970-datasheet
[c] https://navspark.mybigcommerce.com/content/PX1122R_DS.pdf
[d] https://www.septentrio.com/en/node/294/asterx-m3-pro
[e] http://wds-us.com/PDF/NetR9.pdf
[f] https://www.unavco.org/projects/project-support/polar/support/R7.pdf.

adopting the Trimble NetR9. We coupled an OGRE alongside this fixed station to evaluate static positioning performance relative to this well-tested commercial geodetic receiver.

3.2 Battery and reliability

Due to the low strain rates and snow accumulations in the Summit region, each of the 12 static stations established for battery and reliability evaluation was configured to log data at 1 Hz for 24 h on specified days twice a month, corresponding with overflights from the Ice, Cloud, and land Elevation Satellite (ICESat-2) laser altimeter as part of a future inter-comparison study. We determined that a single 12 V/40 Ah AGM battery combined with a 10 W solar panel would power this system throughout the year, based on a 0.63 W total active power consumption and 1.0 mW total sleep power consumption, measured in a laboratory setting. Each station was deployed with this lightweight configuration (totalling 430 USD excluding the instrument) and buried just below the surface, with only the solar panel and GNSS antenna mounted on a pole above the surface as shown in Figure 3.

The following year, each of the 12 stations was excavated in May or June and found to have a fully charged battery, while all files were successfully logged as programmed without the instrument entering low battery mode.

3.3 Data processing

For all GNSS position data processing, we convert the binary messages of the Trimble or OGRE to RINEX using RTKLIB, an open source package for a variety of GNSS data processing functions (www.rtklib.com). We then provided these RINEX files to the Canadian Spatial Reference System Precise Point Positioning (CSRS-PPP) service for online processing using kinematic or static precise point positioning. Data are processed in CSRS-PPP using final IGS orbit solutions and include a 7.5 degree elevation angle cutoff for multipath mitigation, and final solutions are corrected for solid Earth and polar tides. As CSRS-PPP only uses GPS and GLONASS, all other constellations were ignored. CSRS-PPP also only attempts to fix integer phase ambiguities with GPS signals. Solutions are referenced to the GRS80 ellipsoid in the ITRF2020 frame in the epoch of the data, while IGS antenna phase center offset corrections are applied for the calibrated antennas when available. The u-blox ANN-MB antenna used with the OGRE in the kinematic evaluations does not have these corrections. This degrades the solution quality of the OGRE slightly, and while it is difficult to quantify the extent, we know that the phase center offsets increase the uncertainty in the position solution by no more than 9 mm vertically, while the lack of phase center variation corrections increases the error in tropospheric estimates and varies by no more than 5 mm in L1 and 10 mm in L2 (https://content.u-blox.com/sites/default/files/documents/ANN-MB_DataSheet_UBX-18049862.pdf). For these OGRE data, we correct the PPP-produced vertical positions to a pseudo-antenna reference point by subtracting 9 mm from all data.

3.4 Kinematic performance

3.4.1 Instrument precision

Since 2007, a survey of a 15 km snow transect has been conducted on a monthly or bimonthly basis, using a Trimble R7 receiver (Siegfried and others, 2011; Brunt and others, 2017). We assess instrument precision and the relative accuracy by integrating an OGRE alongside this Trimble R7. To not interfere with the R7 setup, we coupled an additional sled that contains the OGRE and a u-blox ANN-MB low-cost 3.3 V LNA antenna (Fig. 4).

Along the 15 km survey, there are 121 designated points where the surveyors typically stop for at least 7 s, in addition to the arbitrary locations in which the surveyors idle for a variety of reasons. At these locations, referred to as pseudo-static points (PSPs), we can assess the precision of each instrument by calculating the horizontal and vertical variability. We take the survey-wide mean value of the PSP 1-sigma values for each instrument, with results shown in Table 2. This method of assessing precision provides a realistic picture of both instruments' performance in this environment with the kinematic data processing technique, mirroring the method used by Siegfried and others (2011). From these results, OGRE precision in both the vertical and horizontal

https://doi.org/10.1017/jog.2023.97 Published online by Cambridge University Press

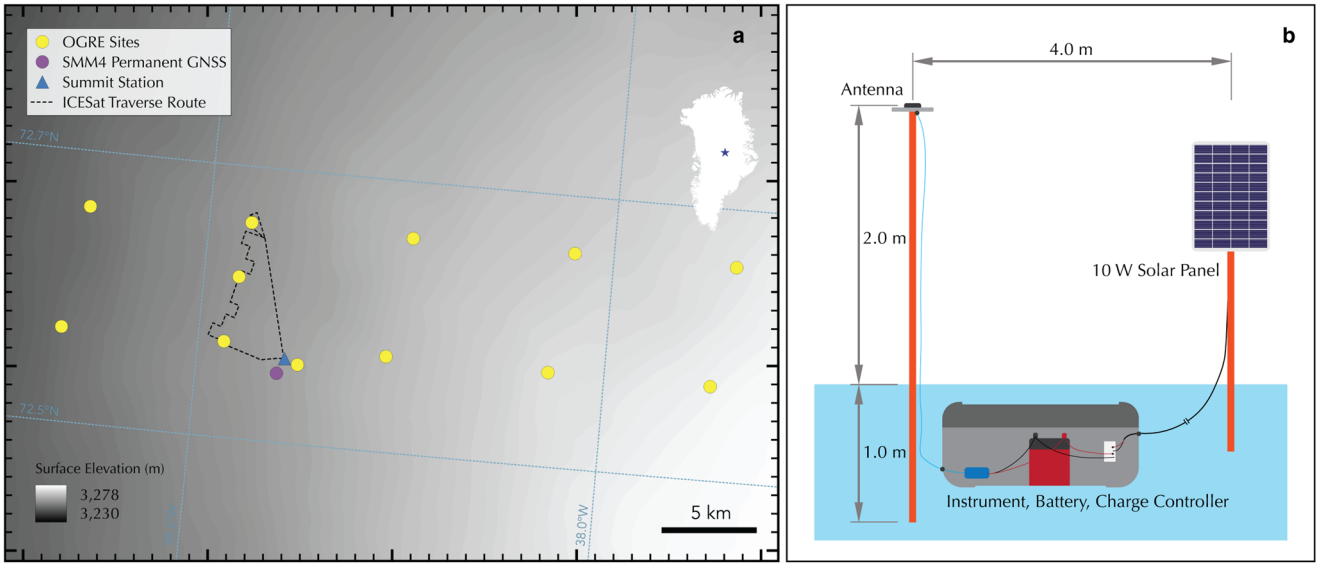

Figure 3. (a) Map of the 12 on-ice OGRE stations deployed for our overwinter testing, along with the location of the ICESat-2 traverse route used in the kinematic evaluation and the location of the SMM4 permanent GNSS station, used in the static evaluation. (b) OGRE station configuration illustration as deployed for the 12 station array, with a 10 W solar panel and a u-blox ANN-MB antenna mounted above ground, and the OGRE, battery and charge controller buried in a protective case below the surface. In this configuration, the cost of materials for the instrument amounted to 200 USD, and the external equipment amounted to 430 USD.

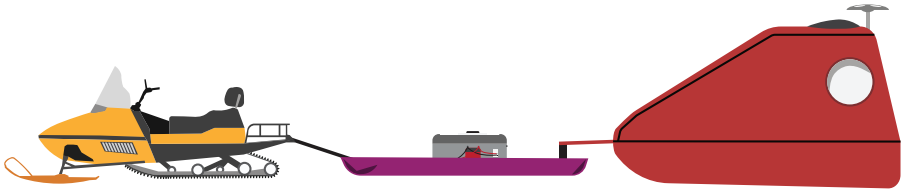

Figure 4. To supplement the standard survey sled (right) employed in the ICESat transect traverse described in Siegfried *et al.* (2011), we coupled an additional sled (left) housing the OGRE and its own low-cost antenna, mounted atop the gray enclosure.

Table 2. Mean PSPs for each instrument across several surveys

	OGRE			Trimble R7		
Date	Horizontal (cm)	Vertical (cm)	N	Horizontal (cm)	Vertical (cm)	N
2022-09-08	0.4	1.1	98	0.3	1.0	102
2022-11-08	0.4	1.4	129	0.4	1.3	128
2022-12-08	0.4	1.2	129	0.3	0.9	129
2023-03-08	0.3	1.3	57	0.4	1.0	57
2023-04-08	0.3	0.8	84	0.3	0.6	84

domains is comparable to that of the Trimble R7 and consistent across surveys. Furthermore, we observe no systematic differences of 1-sigma PSPs between the OGRE and the Trimble, aggregated across all surveys in Figure 5.

3.4.2 OGRE to OGRE and Trimble R7 to Trimble R7 accuracies

To assess accuracy, first we examine a special survey conducted on two separate occasions, colloquially referred to as the 'reverse traverse', whereby the standard survey route is immediately driven in reverse upon completion without stopping at PSPs. This allows for the characterization of each instrument and corresponding antenna and sled infrastructure performance using repeat measurements. We compare GNSS elevation data from the standard segment against the reverse segment using a nearest neighbor technique previously used in other GNSS data intercomparisons in Greenland and Antarctica (Brunt and others, 2019). For each elevation datapoint on the standard survey portion, a 1 m horizontal search radius is defined. The nearest return survey datapoint that falls within this radius is identified and used to calculate the vertical difference. Then, the mean residual is calculated for all point pairs found across the entire survey. This analysis is possible because of the relatively low slope and featureless surface at Summit, which minimizes topographic-induced errors between the two segments.

These special surveys occurred twice, once on 2022-08-18 and again on 2022-11-17. Across each survey, the mean residuals for OGRE-OGRE and Trimble-Trimble vary in sign and range from −1.7 to 1.9 cm, with the 1-sigma standard deviation of the residuals for each comparison retaining sub-6 cm values as shown in Table 3. While these residuals are small, they are not zero. We take the variation in the residuals between surveys to encompass the environmental conditions found on the ice sheet, in addition to potential errors induced by the data processing technique, including variations in tropospheric and ionospheric modeling. The positive bias of the OGRE residuals may be attributed to a systematic difference in sled sinkage in the snow between survey segments and measurement error from the antenna reference point to the snow surface. The 1-sigma standard deviations of these residuals encompass a variety of error terms, including variability in sled penetration into the snow throughout the survey, surface roughness, atmospheric errors and multipath and may not capture correlated errors.

3.4.3 OGRE to Trimble R7 accuracies

To assess relative accuracy between the OGRE and Trimble R7, we translate the elevations from both receivers to the snow surface for ease of intercomparison by subtracting the distance from the antenna reference points to the bottom of the sled, whereby

https://doi.org/10.1017/jog.2023.97 Published online by Cambridge University Press

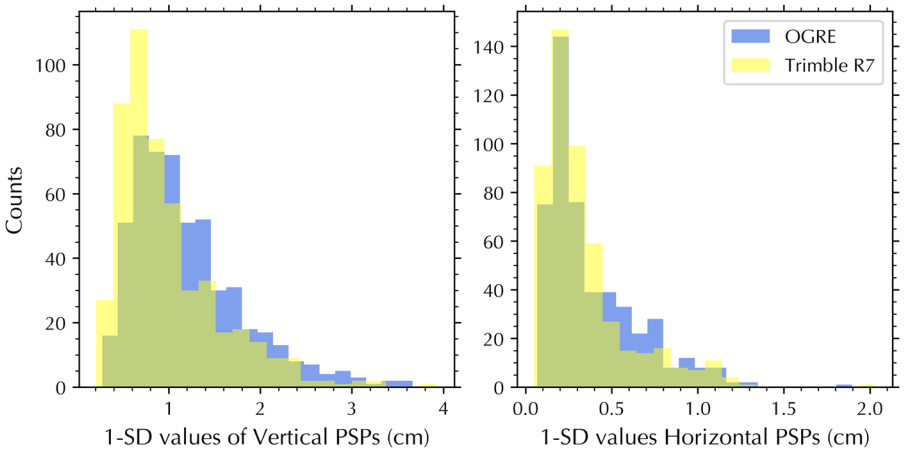

Figure 5. Histogram of vertical (left) and horizontal (right) PSP 1-sigma values aggregated across all surveys, showing that both the OGRE and Trimble have similar-scale precisions. Note that the vertical 1-sigmas tend to be 2.5–3.5 times larger than the horizontal values.

Table 3. Mean vertical difference values of survey instrument combinations for the reverse traverses

Traverse date	Type	Mean residual (cm)	N
2022-08-19	OGRE-OGRE	0.4 ± 3.5	171
	Trimble-Trimble	−1.7 ± 3.3	195
2022-11-17	OGRE-OGRE	0.6 ± 5.4	136
	Trimble-Trimble	1.9 ± 2.9	155

Table 4. Mean vertical difference values between OGRE and Trimble R7 across several ICESat traverses using a 1 m search radius

Traverse date	Mean residual (cm)	N
2022-08-19	−1.3 ± 3.4	6259
2022-09-08	2.2 ± 4.0	2815
2022-11-08	3.8 ± 5.5	4332
2022-11-17	−1.2 ± 4.5	6437
2022-12-08	−1.1 ± 4.8	4831
2023-03-08	−1.1 ± 3.4	1784
2023-04-06	−1.3 ± 3.6	2101

both sleds are generally observed to sink the same vertical distance into the snow. For each elevation datapoint in the OGRE survey, a 1 m horizontal search radius is defined and the same nearest neighbor technique is used as in the previous analysis, with the nearest Trimble R7 datapoint that falls within the horizontal search radius used to calculate the vertical differences. The mean vertical residual is then calculated across the entire survey in Table 4.

Compared to the results from Table 3, the OGRE-Trimble residuals yield similar scale measurements in mean residual and corresponding 1-sigma uncertainties. This indicates that the error characteristics from both evaluations are largely driven by external factors previously identified: topographic variability between instruments, atmospheric effects and multipath. The 1-sigma uncertainties now also capture instantaneous differences in penetration depth of the two sleds, which may ride on the snow surface differently, and the unique internal error characteristics of each receiver. Because of the relatively featureless surface of the survey area, it is hard to distinguish the contributing effect of topography on the residual uncertainties in relation to other sources of error. However, we conclude that both instruments perform comparably in the ice-sheet kinematic environment in which they were tested, with the OGRE elevation consistently falling within 3 cm of the Trimble surface across multiple survey campaigns. When we analyze all residuals across all conducted surveys, we calculate an overall mean residual of −0.1 ± 4.7 cm, with no apparent systematic issues in data processing or instrument performance between the two receivers (Fig. 6).

With this method of receiver intercomparison, it is impossible to assess the relative horizontal accuracy of the OGRE because each instrument occupies a different sled with a different antenna. However, given the intrinsic nature of GNSS constellation geometry that leads to a lower horizontal positioning error than the vertical positioning error on the Earth's surface, we expect the horizontal accuracy of the OGRE to be at least as good as the vertical performance presented above (Tahsin and others, 2015). Ultimately, we take the mean multi-survey residual of −0.1 ± 4.7 cm to demonstrate the relative accuracy of the OGRE

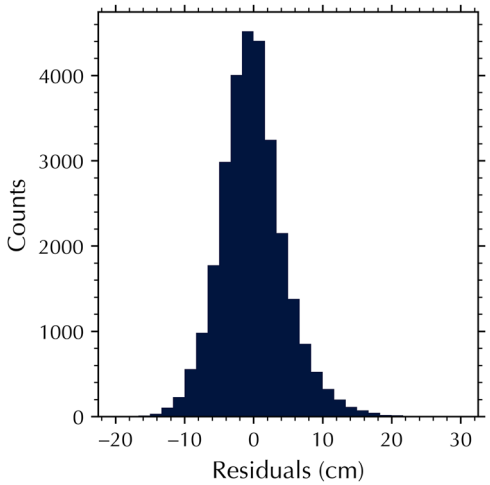

Figure 6. Histogram of OGRE-Trimble R7 vertical residuals aggregated across all surveys.

compared to the Trimble R7, and we use the multi-survey mean of PSPs to define the OGRE precision, with a mean 1-sigma value of 1.2 cm vertically and 0.4 cm horizontally, compared to 1.0 cm vertically and 0.3 cm horizontally for the Trimble R7.

3.5 Static performance

We also conducted a trial to demonstrate instrument performance in a statically processed configuration by determining the simultaneous static-PPP positions of an OGRE and a Trimble NetR9 mounted side-by-side. Once again, we did not interfere with the existing Trimble NetR9 and geodetic antenna setup and instead installed the OGRE nearby with a low-cost TOPGNSS TOP106

https://doi.org/10.1017/jog.2023.97 Published online by Cambridge University Press

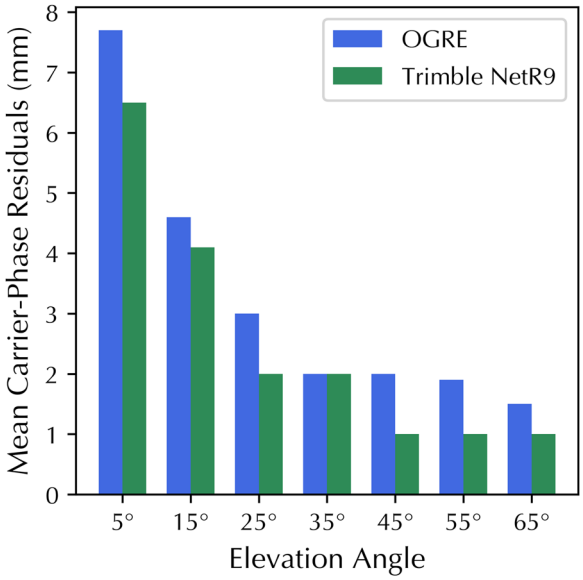

Figure 7. Carrier-phase residuals of the OGRE and Trimble, reported by CSRS-PPP, averaged across all surveys and binned by elevation angle.

multi-band antenna. Because of the dynamic nature of the ice sheet, the building that houses both receivers is estimated to move about 5 mm horizontally per day with the ice sheet, in addition to other unquantified vertical and rotational movements (Hawley and others, 2020). We acknowledge that the quality of any data processed in static mode will be biased by this ice-sheet movement, however some glaciologists choose to assume ice movement as virtually stationary during sufficiently brief periods (King, 2004). By curtailing logging sessions to 12 h, we reduce the effects of movement for the purposes of this trial while still providing enough data to CSRS for millimeter to centimeter-level convergence. To assess the static performance of the OGRE over 11 12 h sessions, we calculate the baseline between the OGRE and the Trimble PPP from each statically processed position pair.

The standard deviation of the baseline distance between both instruments over this period was 2.0 mm. This variability is a representation of the error characteristics of both receivers, with sources of error including formal instrument errors, atmospheric errors and multipath characteristics of the antennas of differing quality. While this trial was of short duration, this millimeter-level uncertainty shows a high degree of relative accuracy between the OGRE and Trimble NetR9 in a static setting.

While the baseline variability does not reveal which instrument is more accurate, we can also examine the measurement quality of each instrument by analyzing the estimated carrier-phase residuals of each device. Figure 7 shows the RMS carrier-phase residuals of the L1W GPS band measured across the range of elevation angles of satellites observed from Summit, and averaged across all surveys. Carrier-phase residuals are the differences in the carrier-phase-based estimated pseudoranges, and are indicative of measurement noise consisting of factors not modeled by PPP, such as multipath and internal receiver signal processing characteristics.

While the Trimble matches or exceeds the performance of the OGRE carrier-phase residuals, we note that these baseline variations are not a comparison of receiver to receiver, but rather system to system: the separate antennas used by each receiver, in combination with the internal signal processing characteristics of each receiver, likely account for these differences. Nonetheless, these results show that a low-cost instrument, the OGRE, combined with a low-cost antenna, has comparable performance in measurement quality to a permanent geodetic-grade base station.

4 Discussion and conclusions

4.1 Discussion

The results presented here encompass various modes of operation of a GNSS receiver that glaciologists may use to study the cryosphere. The OGRE, in combination with two separate low-cost antennas, has shown comparable performance characteristics across precision and accuracy evaluations in the prescribed icy environment. By using low-cost antennas across our tests with the OGRE, there is a reduction in measurement quality, but the low multipath and open-sky environment of glaciers and ice sheets may reduce the need for the same signal processing capabilities of traditional geodetic receivers. Furthermore, there are significant cost savings in a patch antenna of this style and our results showed that in conjunction with an OGRE, the entire system can perform well. Other studies now demonstrate that it is also possible to implement field corrections for the u-blox ANN-MB, or even generate industry standard ANTEX files, however this is beyond the scope of this paper (Krietemeyer and others, 2022).

Beyond the cost reductions by using the antennas presented in this paper, the overall cost reduction of the OGRE, both in material price and corresponding station hardware (batteries, solar panel, housing), allowed us to install the 12 station arrays at Summit in just 3 d and with a team of three. Logistics were further simplified by the total 22.5 kg weight of the instrument, battery and other requisite equipment, a significant reduction in material weight, while configuration time and logistics were also simplified in the field.

4.2 Conclusions

We have presented an analysis on the performance of a novel, multi-GNSS instrument designed for autonomous, long duration measurements in remote regions of the cryosphere. Totaling approximately 200 USD in material costs (excluding the antenna) and consuming just 0.63 W when tracking multiple constellations with a u-blox ANN-MB or TOPGNSS TOP106 antenna and logging at 1 Hz, this instrument vastly reduces the cost and logistical challenges of deploying GNSS instrumentation to remote regions. With these improvements, more GNSS instruments can be deployed in a single campaign, thereby increasing the spatial resolution of the GNSS survey. We have also made the OGRE simple to configure and customize with our open source hardware and software. External connections allow for the addition of satellite or radio telemetry, or the interface of additional sensors.

In conjunction with precise point positioning data processing techniques and a low-cost antenna, we showed that OGRE test results are both self-consistent and agree closely with existing kinematic and static positioning methods employed in the Summit region. For the kinematic trials, the overall OGRE residual compared to the Trimble R7 is -0.1 ± 4.7 cm, while the 1-sigma PSPs are 1.2 cm vertically and 0.4 cm horizontally. For the static trial, the baseline 1-sigma value against the Trimble NetR9 is 2.0 mm, with comparable carrier phase residuals. We also deployed a static array of OGREs to demonstrate the capabilities of this instrument in long-term positioning in a harsh environment, showing robust battery performance in this configuration, with all stations able to carry out their programmed configuration of logging twice a month for 24 h without depleting the battery.

https://doi.org/10.1017/jog.2023.97 Published online by Cambridge University Press

Data. Monthly RINEX Trimble R7 and OGRE data as part of our kinematic analysis, along with OGRE and NetR9 (SMM4) data used in the static evaluation, are available publically at https://doi.org/10.18739/A29K45V2K. Static base station (SMM4) data are also available from Earthscope https://doi.org/10.7283/EBJP-VE93. For software code and hardware design, visit www.github.com/glaciology/OGRENet.

Acknowledgements. We thank J. Renk and J. Wilner for their support and feedback in the design and the deployment of the OGREs, respectively. We also thank Polar Field Services and Battelle ARO for field support logistics. This project was funded by the US National Science Foundation Office of Polar Programs grant #2028421.

References

Brunt KM and 7 others (2017) Assessment of NASA airborne laser altimetry data using ground-based GPS data near Summit Station, Greenland. *The Cryosphere* **11**(2), 681–692. doi: 10.5194/tc-11-681-2017

Brunt KM, Neumann TA and Larsen CF (2019) Assessment of altimetry using ground-based GPS data from the 88S Traverse, Antarctica, in support of ICESat-2. *The Cryosphere* **13**(2), 579–590. doi: 10.5194/tc-13-579-2019

Brunt KM, Smith BE, Sutterley TC, Kurtz NT and Neumann TA (2021) Comparisons of satellite and airborne altimetry with ground-based data from the interior of the Antarctic Ice Sheet. *Geophysical Research Letters* **48**(2), e2020GL090572. doi: 10.1029/2020GL090572

Castellani BB, Shupe MD, Hudak DR and Sheppard BE (2015) The annual cycle of snowfall at Summit, Greenland. *Journal of Geophysical Research: Atmospheres* **120**(13), 6654–6668. doi: 10.1002/2015JD023072

Dunse T, Schuler TV, Hagen JO and Reijmer CH (2012) Seasonal speed-up of two outlet glaciers of Austfonna, Svalbard, inferred from continuous GPS measurements. *The Cryosphere* **6**(2), 453–466. doi: 10.5194/tc-6-453-2012

Hamza V, Stopar B and Sterle O (2021) Testing the performance of multi-frequency low-cost GNSS receivers and antennas. *Sensors* **21**(6), 2029. doi: 10.3390/s21062029

Hansen K and 13 others (2021) Estimating ice discharge at Greenland's three largest outlet glaciers using local bedrock uplift. *Geophysical Research Letters* **48**(14), e2021GL094252. doi: 10.1029/2021GL094252

Hawley RL, Neumann TA, Stevens CM, Brunt KM and Sutterley TC (2020) Greenland ice sheet elevation change: direct observation of process and attribution at summit. *Geophysical Research Letters* **47**(22), e2020GL088864. doi: 10.1029/2020GL088864

Jones DH, Robinson C and Gudmundsson GH (2016) A new high-precision and low-power gnss receiver for long-term installations in remote areas. *Geoscientific Instrumentation, Methods and Data Systems* **5**(1), 65–73. doi: 10.5194/gi-5-65-2016

Khan SA and 9 others (2022) Extensive inland thinning and speed-up of Northeast Greenland Ice Stream. *Nature* **611**(7937), 727–732. doi: 10.1038/s41586-022-05301-z

King M (2004) Rigorous GPS data-processing strategies for glaciological applications. *Journal of Glaciology* **50**(171), 601–607. doi: 10.3189/172756504781829747

Krietemeyer A, van der Marel H, van de Giesen N and Veldhuis MC (2022) A field calibration solution to achieve high-grade-level performance for low-cost dual-frequency GNSS receiver and antennas. *Sensors* **22**(6), 2267. doi: 10.3390/s22062267

Larson KM, MacFerrin M and Nylen T (2020) Brief communication: update on the GPS reflection technique for measuring snow accumulation in Greenland. *The Cryosphere* **14**(6), 1985–1988. doi: 10.5194/tc-14-1985-2020

Mitchell CN and 5 others (2005) GPS TEC and scintillation measurements from the polar ionosphere during the October 2003 storm. *Geophysical Research Letters* **32**(12), L12S03. doi: 10.1029/2004GL021644

Möller D and Ritter B (1988) Glacial geodetic contributions to the mass balance and dynamics of ice shelves. *Annals 341 of Glaciology* **11**, 89–94. doi: 10.3189/S0260305500006388

Siegfried MR, Hawley RL and Burkhart JF (2011) High-resolution ground-based GPS measurements show intercampaign bias in ICESat elevation data near Summit, Greenland. *IEEE Transactions on Geoscience and Remote Sensing* **49**(9), 3393–3400. doi: 10.1109/TGRS.2011.2127483

Still H and 10 others (2022) Tidal modulation of a lateral shear margin: Priestley Glacier, Antarctica. *Frontiers in Earth Science* **10**. doi: 10.3389/feart.2022.828313

Tahsin M, Sultana S, Reza T and Hossam-E-Haider M (2015) Analysis of dop and its preciseness in GNSS position estimation. In *2015 International Conference on Electrical Engineering and Information Communication Technology (ICEEICT)*, pp. 1–6.